Nucleic Acids Research, 1999, Vol. 27, No. 19 **3945–3952**

Accurate selection of a 5' splice site requires sequences within fibronectin alternative exon B

Bruce A. Kuo and Pamela A. Norton*

Department of Medicine, Division of Gastroenterology and Hepatology, Thomas Jefferson University, Philadelphia, PA 19107, USA

Received April 5, 1999; Revised July 12, 1999; Accepted August 12, 1999

ABSTRACT

Inclusion of fibronectin alternative exon B in mRNA is developmentally regulated. Here we demonstrate that exon B contains two unique purine-rich sequence tracts, PRE1 and PRE2, that are important for proper 5' splice site selection both *in vivo* and *in vitro*. Targeted mutations of both PREs decreased the inclusion of exon B in the mRNA by 50% *in vivo*. Deletion or mutation of the PREs reduced removal of the downstream intron, but not the upstream intron, and induced the activation of cryptic 5' splice sites *in vitro*. PRE-mediated 5' splice selection activity appears sensitive to position and sequence context. A well characterized exon sequence enhancer that normally acts on the upstream 3' splice site can partially rescue proper exon B 5' splice site selection. In addition, we found that PRE 5' splice selection activity was preserved when exon B was inserted into a heterologous pre-mRNA substrate. Possible roles of these unique activities in modulating exon B splicing are considered.

INTRODUCTION

Fibronectin is an extracellular matrix protein which is important for cellular adhesion. The genomic structure and gene expression of fibronectin has been conserved in chicken, mouse, rat and human; the gene contains more than 40 exons (1). Multiple isoforms of the fibronectin protein are produced during development via alternative splicing of three exons (A, B and V) within the pre-mRNA (2). Fibronectin exon B is generally excluded in adult and differentiated tissues. Previous studies have shown that exon B exclusion appears to be a default pathway due to a combination of weak splice sites, branch sites and an unusual polypyrimidine tract (3,4). Sequences within the downstream intron (IVS2) or exon B itself were found to be required for exon B inclusion (5–7). However, the mechanisms by which these sequences influence exon B splice site selection is not well understood.

The process by which constitutive and alternative exons are recognized in a pre-mRNA is complex. Conserved sequences near the 3' and 5' splice sites are generally sufficient to signal the assembly of small ribonuclear proteins (snRNPs U1, U2, U4/U5/U6) and many non-snRNP components into an active spliceosome (reviewed in 8–10). The strength of a 5' splice site is largely determined by its ability to base-pair with the 5' end of U1 snRNA (11), as reflected in the consensus sequence 5'-CAG/GTGAGT-3'. This interaction is an early step in committing a 5' splice site to spliceosomal assembly. In addition, sequences within some alternative exons are required for accurate splicing (12–18). Such exon sequences frequently are characterized by short purine-rich tracts (6–12 nt). Sequences that inhibit exon recognition also have been identified (19–21). *Cis*-elements that act as exon sequence enhancers (ESEs) or silencers may function by interactions with soluble factors such as members of the family of SR proteins (22,23).

Exon recognition is currently understood to involve interaction between the 3' and 5' splice sites that flank the exon (24). For instance, inclusion of alternative exon 4 of preprotachykinin involves the cooperative assembly of U1 at the 5' splice site and U2AF65 at the upstream polypyrimidine tract (25). In principal, exon sequences could play a role in such bridging interactions by providing binding sites for factors such as SR proteins, which in turn interact with factors bound at splice sites flanking an exon (26). Because exon B has such weak splice sites, we have explored such an expanded role for exon B sequences.

Here we report the presence of two purine-rich elements (PRE1 and PRE2) within exon B which contribute to accurate selection of the 5' splice site *in vivo* and *in vitro*. PRE splice site selection activity showed both position and context dependence. Substitution of either the 3' or 5' exon B splice site largely stimulated removal of the associated intron and not the other. The participation of exon sequences in proper 5' splice site selection appears to be a novel activity that is separable from other characterized exon sequence functions.

MATERIALS AND METHODS

Splicing substrate construction

The rat FN splicing substrates were derived from the 7B8 and 7iBi89 mini-genes (3,4). The FN1 substrate (Fig. 1A) consists of exons III7b, EIIIB and III8a (herein referred to as exons 7, B and 8), intron IVS1 with a 1.1 kb internal deletion, complete intron IVS2, and 260 bp of intron IVS3 (details of plasmid constructions are available upon request). The shortened IVS1 (184 nt) facilitated detection of IVS1-containing RNAs. IVS2

*To whom correspondence should be addressed at: Thomas Jefferson University, 365 JAH, 1020 Locust Street, Philadelphia, PA 19107, USA. Tel: +1 215 503 1622; Fax: +1 215 923 7697; Email: pnorton@lac.jci.tju.edu

Table 1. Primer sequences

BF primers	
KasF	AGAGGCGCCCCAGCTCACTGACC
RBF3	CCTAAGCTTTGTTGATATAACTG
RBF	TACCGAATCACAGTAGTTGC
P1F	CGAATCACAGTAGTTGCGGCAGCTCTAGG
P2F	ATGGCGGTCTCAGTGCCCCTAC
BR primers	
SgR	CAAGATTCACCGGTGGCTGTGTCAGTG
RBR	GGTCCACCTCAGGCCGATGC
P1R	GATCCCTAGAGCTGCCGCAACTACTGTGATTCGGTAC
P2R	GCACTGAGACCGCCATTAATGA
8R primers	
R8R	GGTGAATCGCAGATCCGTGG
R8R2	ACCCGCATAGTGTCCGGACC
RM8a2	GGTGAGTAGCGCACCAAGAG
Other primers	
7F	CATGCCGATCAGAGTTCCTG
IVS2R	ATCCCCATGGCCAATCGCTGGCTTC
I2RT7	TAATACGACTCACTATAGGGCGAACATGGCCAATCGCTGGCTTC
IVS3R	GATAAGTGTCTACTGAACC

(1071 nt) was not shortened due to the presence of *cis*-elements necessary for splicing (5); this rendered IVS2-containing mRNAs undetectable by RT–PCR. The exon 8 5' splice site was included to facilitate exon recognition (27). Unique *Kas*I and *Sgr*AI restriction sites were introduced into the 5' and 3' ends of exon B, respectively, by PCR using the primers KasF and SgR (Table 1).

To generate FN3, the exon B branch points, polypyrimidine tract and 3' splice site were replaced with 90 bp of the equivalent region of an adenovirus intron plus 19 bases of the adjacent exon from pPiP3 (28) (kind gift of M. Garcia-Blanco). A consensus 5' splice site was inserted into the *Sgr*AI site of exon B in FN1 and FN3 to create FN5 and FN3.5 (5'-CCG/GTGAAT-3' within the *Sgr*AI site was altered to 5'-CCG-GCAG/GTGAGTACCG/GTGAAT-3'). The intact, wild type exon B 5' splice site remains 10 bases downstream.

Deletions within exon B were generated in FN1, FN3 and FN5 by use of available restriction sites (Figs 1 and 4). To generate FN1ΔBS40, a 40 bp *Bgl*II/*Bam*HI polylinker fragment from pSP72 (Promega) was ligated at the *Bam*HI/*Sgr*AI sites. The FN3mp construct was assembled by PCR in a multi-step process using primer pairs KasF/P1R, P1F/SgR, 7F/P2R and P1F/IVS2R (Table 1). FN1cp and FN1ΔBScp were generated by ligating an optimized cTNT exon 5 enhancer [5'-AGCTTA-AGAGGAAGAAGAAGAAGAGGAAGTCGA-3' (29)] into the exon B *Hin*dIII site of FN1 or into the *Eco*RV site of FN1ΔBS40, respectively.

AdFN contains 150 bases of IVS1, all of exon B from FN1 and 80 bases of IVS2 inserted into the *Xba*I site of pAd8i. pAd8i was generated by insertion of 150 bases of exon 8 and 260 bases of IVS3 into the *Hin*dIII site of pPiP3. Versions of the AdFN plasmid containing deletions within exon B were generated from the corresponding deletion plasmids.

Exon B-containing pre-mRNA templates used in transfection studies were generated by ligating inserts from the FN1, FN3, FN3mp and FN5 plasmids into the blunted *Bam*HI site of the eukaryotic expression vector pBAGH (3).

Transfection of F9 cells and RNA isolation

F9 cells (ATCC–CRL1720) were cultured as suggested by the supplier. Transfections were performed using Lipofectamine Reagent (Gibco BRL). Total RNA was isolated 48 h later using TRIzol (Gibco BRL) (30) and resuspended in 10 µl of water.

Pre-mRNA and RNA probe synthesis

Pre-mRNAs were synthesized with T7 RNA polymerase (Stratagene) as suggested by the manufacturer and quantitated by optical density at 260 nm. Probes for the RNase protection assay were synthesized in the presence of 50 µCi [α-^{32}P]UTP or -CTP (800 Ci/mmol). Transcripts were purified by denaturing acrylamide gel electrophoresis or by Sephadex G-50 spin-column fractionation.

Nuclear extract and SR protein isolation and *in vitro* splicing reactions

Nuclear extracts were prepared from about 4×10^9 HeLa cells (Cell Culture Center, Minneapolis, MN) (31). Total SR proteins were isolated from about 10^{10} HeLa cells (32). SR proteins were reconstituted at 10 µg/µl in buffer D.

A standard 25 µl splicing reaction contained 50 fmol of pre-mRNA, 10 µl of HeLa nuclear extract, 10 mM HEPES (pH 7.6), 5 mM creatine phosphate, 1.6 mM ATP, 3 mM $MgCl_2$ and 1 U of RNaseBlock. Incubation was at 30°C for 2 h. Spliced products were recovered as described (4) and resuspended in 20 µl of water. Where indicated, SR proteins were added to the reaction mix after addition of nuclear extract and prior to addition of pre-mRNA. For each combination of nuclear extract and SR protein preparation, the latter was titrated to establish the amount of SR protein needed to activate FN1 splicing. The amount of SR protein used is stated for each experiment.

RT–PCR assay

Reverse transcription (RT) of spliced products was performed with Superscript II MoMLV reverse transcriptase (Gibco BRL). One µl of RNA was reverse transcribed using primer RM8a2 or IVS3R. Amplification conditions were as suggested for *Taq* DNA polymerase (Stratagene); 25 cycles, unless otherwise specified, consisting of 1 min at 94°C, 1 min at 58°C and 30 s at 72°C.

As a result of the altered structure of the central exon B in some substrates, different exon B primers were required to detect spliced products (Table 1). All exon B forward and reverse primers amplified a single target with comparable efficiency (data not shown), accurately reflecting the differences in the amount of the spliced substrate. Table 1 lists the primers used interchangeably as BF, BR and 8R. PCR products were separated on 5% acrylamide (TBE) gels and visualized by ethidium bromide staining. Gels were photographed; scanned images were contrast inverted and analysis was performed using NIH Image (ftp from zippy.nimh.nih.gov).

RNase protection

RNase protection probes were transcribed using T7 RNA polymerase from a PCR fragment generated with forward primer 7F and return primer I2RT7 (T7 promoter-containing). The FN1 and FN5 templates were truncated at the *Eco*NI site in IVS1, while FN3, FN3.5 and FN3mp were truncated at the *Xba*I site in pPiP3. RNase protection assays were performed as previously described (33). Results represent a minimum of four experiments.

RESULTS

Exon B splicing *in vivo*

The minigene FN1 contains exon B with flanking introns and exons. Internal truncation of the upstream intron, IVS1, and point mutations introduced near the ends of exon B to facilitate subsequent manipulations had no effect on splicing (data not shown). FN1 and other FN minigenes were transiently introduced into F9 mouse embryonal carcinoma cells (34), which express a high percentage of exon B containing (B+) fibronectin mRNA (3). Total RNA from transfected cells was analyzed by RT–PCR. Primer IVS3R, which recognizes the rat-derived minigene RNA but not the related endogenous mouse mRNA (data not shown), was used for reverse transcription, and with primer 7F for amplification (Fig. 1A). Approximately 5% of the total spliced material contained exon B (B+ mRNA) (Fig. 1, lane 1), whereas 80% of the endogenous FN mRNA was B+ (data not shown). A bias toward B– mRNA in transiently transfected cells was reported previously (3). Improvement of either 3' or 5' splice site flanking exon B (FN3 and FN5) resulted in nearly 100% B+ mRNA (Fig. 1, lanes 4 and 6). Exclusive use of the improved FN5 5' splice site was confirmed by restriction analysis.

To evaluate the role of exon B sequences, exon B was subdivided: the upstream half (FN1ΔKB) or the downstream half (FN1ΔBS) (Fig. 1A). For FN1ΔKB, both B+ (40% of spliced product) and B– forms were generated (Fig. 1B, lane 2). This increase relative to FN1 suggested that sequences within the deleted region (i) suppress 3' splice site use, (ii) move a positive element to a position that favors use of the 3' splice site or (iii) decrease the large exon B (272 nt) to a length that is more easily spliced. We regard the last possibility as unlikely since similarly sized FN1ΔBS eliminated exon B inclusion (lane 3). Thus, the FN1ΔKB deletion appears to either remove a negatively acting element or reposition a positive element.

Visual inspection of exon B sequences identified two purine-rich sequence tracts which we refer to as PRE1 (5'-AGGAGAAGGGA-3'), located just upstream of the *Bam*HI site, and PRE2 (5'-GGAGAGAG-3'), located ~30 nt upstream of the 5' splice site. As purine-rich elements act as ESEs in other exons (35), we tested whether PRE1 and PRE2 function in this fashion for exon B. Transversion mutations were introduced into each PRE in the FN3 context to see if the high level of B+ mRNA could be reduced (Fig. 1A, FN3mp and Fig. 4B). FN3mp showed reduced exon B inclusion relative to FN3 (Fig. 1A, lanes 4 and 5), indicating that the PREs possess enhancer-like activity. Analysis of an additional unexpected product by restriction mapping and sequencing revealed that a cryptic 5' splice site, EC, was activated (5'-CGG/GTACCG-3'). Thus, *in vivo* results show that exon B sequences affect exon B recognition, and activation of the cryptic 5' splice site suggests a role for PREs in correct 5' splice site selection.

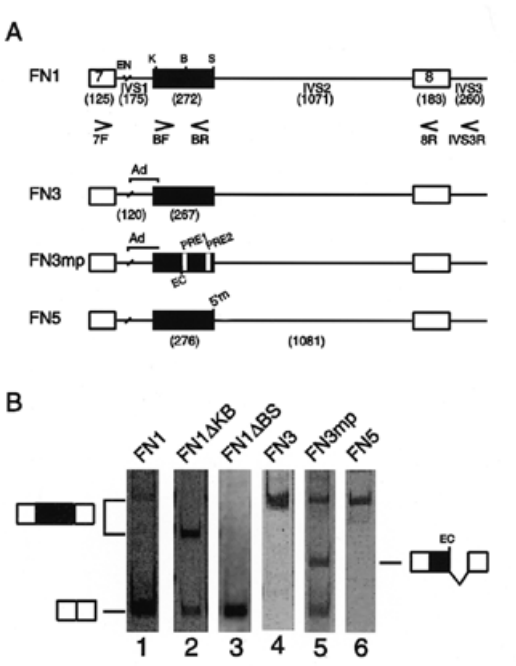

Figure 1. Mutational analysis of exon B in transfected F9 cells. (**A**) Structure of exon B-containing pre-mRNAs. Filled boxes, exon B; open boxes, exons 7 or 8; lines, introns. Relevant restriction endonuclease sites: EN, *Eco*NI; K, *Kas*I; B, *Bam*HI; S, *Sgr*AI. FN1, native fibronectin splice sites; FN3, adenovirus 3' splice site region (bracket); FN5, consensus 5' splice site; FN3mp, mutations in the purine-rich elements. Primers used in RT–PCR analyses are indicated by arrows. (**B**) RT–PCR detection of B+ and B– mRNAs. Spliced products were detected in total RNA by RT–PCR using primers 7F and IVS3R. Both B+ (upper band) and B– (lower band) forms were detectable. Amplification was for 35 cycles. The middle band generated by the FN3mp substrate (lane 5) represents use of a cryptic 5' splice site in exon B, indicated at right. This is a contrast-inverted image of an ethidium bromide-stained gel. FN1ΔKB, sequences deleted between *Kas*I and *Bam*HI sites; FN1ΔBS, sequences deleted between *Bam*HI and *Sgr*AI sites.

Introns flanking exon B require different conditions for *in vitro* splicing

The mechanisms by which exon B 3' or 5' splice site substitution activated exon B inclusion in F9 cells (this study) and in HeLa cells (3) are not clear. An *in vitro* splicing system was developed to monitor splicing of the individual introns flanking exon B. Initially, pre-mRNA FN1 was incubated in a standard splicing reaction containing HeLa nuclear extract. Splicing products were reverse transcribed and amplified with various primers. Using primers 7F and 8R the B– product appeared as a faint band (Fig. 2A, lane 1), but the B+ product was not detected. No IVS1 removal was detected using primers 7F/BR (Fig. 2B, lane 1), in agreement with our earlier studies (4,36). No IVS2 removal was detected using primers BF/8R (Fig. 2C, lane 1). Thus, HeLa nuclear extract alone did not support the low level of exon B inclusion that occurs in HeLa cells *in vivo* (3,37).

Because SR proteins can promote certain alternative splicing events (38,39), SR proteins purified from HeLa cells were

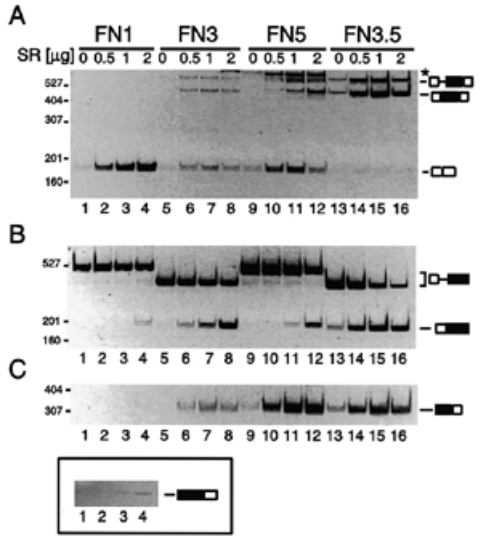

Figure 2. *In vitro* splicing of FN pre-mRNAs. Pre-mRNAs FN1, FN3, FN5 (diagrammed in Fig. 1A) and FN3.5 (incorporates modifications of both FN3 and FN5) were incubated in HeLa nuclear extract with varying amounts of SR proteins added as indicated at the top. Spliced products were detected by RT–PCR; see Figure 1A for primers. Molecular size markers are noted to the left of each panel. Product structures are indicated to the right of each panel; filled box, exon B. Semi-quantitative comparisons are made between products derived from different substrates that were incubated under identical conditions. (**A**) B+ and B− mRNA detection with primers 7F/8R. Asterisk (*), aberrant/unspliced products. (**B**) IVS1+ and IVS1− mRNA detection with primers 7F/BR. (**C**) IVS2− mRNA detection with primers BF/8R. Lanes 1–4, boxed, amplification using double the amount of template. This is a contrast-inverted image of an ethidium bromide-stained gel.

titrated into splicing reactions. An increase in joining of exons 7 and 8 (Fig. 2A, lanes 2–4) suggested a general stimulation of splicing, but the three exon product was not detected. We found that the 7–B product could be detected (Fig. 2B, lane 4) but the B–8 product was only detected using twice the amount of cDNA template in the amplification process (Fig. 2C, lanes 2–4, and boxed). Thus, addition of SR proteins stimulated all splicing reactions of the FN1 substrate including 7–8 joining as well as 7–B and B–8 splicing.

Analysis of 7–B and B–8 products revealed that the two introns were activated at different concentrations of added SR proteins. IVS1 removal required relatively high levels of SR proteins, with efficient splicing even at higher levels than those shown. In contrast, stimulation of IVS2 splicing (and 7–8 joining) occurred at the lower range of added SR proteins. At higher levels of SR proteins (5–10 μg) correct IVS2 removal sometimes yielded to formation of larger products >900 nt (data not shown), representing aberrant/unspliced products. However, by supplementing HeLa nuclear extract with various amounts of SR proteins, the *in vitro* system appears to reproduce all the possible splicing products that pre-mRNA FN1 can generate *in vivo*.

Improved exon B 3' or 5' splice sites promotes splicing of IVS1 or IVS2

Both FN3 and FN5 produced high levels of B+ mRNA *in vivo* (Fig. 1). Similar results were not reproduced *in vitro*; only very low levels of B– mRNA were produced from either pre-mRNA (Fig. 2A, lanes 5 and 9). Thus, the improved splice sites were not sufficient to drive exon B inclusion in HeLa nuclear extract. However, splicing of FN3 or FN5 in HeLa extract containing SR proteins produced B+ mRNA (Fig. 2A, lanes 6–8 and 10–12). Densitometric analysis of this semi-quantitative assay indicated that the B+ form represents up to 30% of total FN3 spliced products and up to 60% of total FN5 spliced products. Exclusive use of the consensus 5' splice site in FN5 and not the native site was confirmed by sequencing. Thus, both splice site substitutions increased exon B inclusion.

The mechanisms by which the splice site improvements stimulated exon inclusion were explored by analyzing splicing of the individual flanking introns. The short length of IVS1 permits direct quantitation of the spliced (IVS1–) mRNA and unspliced (IVS1+) pre-mRNA. The native exon B 3' splice site of FN5 was spliced more efficiently than the same site in FN1 (20% conversion of IVS1+ to IVS1– for FN5 versus 10% for FN1). However, the improved 3' splice site of FN3 was considerably more active in stimulating IVS1 removal (40%, and compare Fig. 2B, lanes 4, 8 and 12). The longer IVS2-containing RNAs are not reliably detected in this system. However, the improved 5' splice site of FN5 appeared to have a greater effect on IVS2 splicing than the 3' splice site substitution of FN3, based on the relative amounts of accumulated product (Fig. 2C, lanes 5–12). Thus, in both instances, the splice site substitutions appeared to act primarily by stimulating splicing of the intron in which they reside.

RNase protection provided a means of quantitating the splicing efficiency of IVS1 and IVS2 simultaneously and comparing the efficiency of splicing of the different substrates. RNA probes that included all of exon B and portions of IVS1 and IVS2 were prepared for each substrate (Fig. 3A). Splicing of either IVS1 or IVS2 was not detected in FN1 splicing reactions (Fig. 3B, lane FN1); faint bands smaller than that protected by unspliced RNA are not spliced products as they are present in reactions that lack ATP (data not shown). Analysis of FN3 confirmed the efficient removal of IVS1 detected by RT–PCR. The absence of RNAs in which IVS2 alone was spliced suggests that the fully spliced FN3 product was generated via sequential removal of IVS1 then IVS2 (Fig. 3B, lane FN3). Analysis of FN5 confirmed the efficient splicing of IVS2 detected by RT–PCR. However, IVS1 splicing remained inefficient under these conditions, resulting in little fully spliced exon B (Fig. 3B, lane FN5). Thus, the principle effect of each weak splice site is to limit splicing of the intron that includes the site.

One formal possibility is that other elements restrict exon B inclusion, such as inhibitory sequences within the exon. However, splicing of doubly substituted pre-mRNA FN3.5 resulted in a high level of B+ mRNA, with very little B– mRNA detected (Fig. 2A, lanes 13–16 and Fig. 3B, lane FN3.5). These results suggest that exon B sequences do not prevent efficient exon inclusion if both weak splice sites are improved.

Exon B deletions influence IVS2 5' splice site selection

To further examine the role of exon B sequences in exon B recognition, additional deletions were introduced into exon B within FN1. *In vitro* spliced products were analyzed by RT–PCR rather than the less sensitive RNase protection assay. Reactions were supplemented with various levels of SR proteins; the reactions shown represent the conditions that

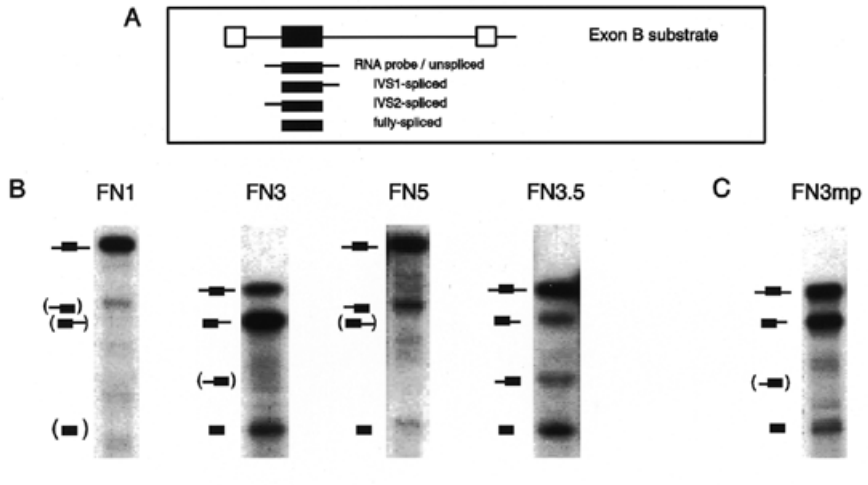

Figure 3. Detection of *in vitro* spliced products by RNase protection. (**A**) The region of probe complementarity is shown below the pre-mRNA; structures of partially protected fragments are shown below the probe and to the left of each panel below. (**B**) RNase protection analysis of spliced products. Levels of splicing activity were comparable to that in Figure 2, lane 3 (5 μg SR proteins were included). RNase-resistant fragments protected by the indicated RNAs were separated on a 4% acrylamide–urea gel, dried and exposed to film. Differences in probe structure account for variation in product size. Parentheses mark the expected location of products that were not detected. (**C**) Analysis of spliced products of FN3mp was as in (B).

produced the maximal amounts of FN1 products. Deletion of exon B sequences had only modest effects on IVS1 splicing, as assessed by the ratios of spliced to unspliced RNAs (Fig. 4A, compare lane 1 with lanes 2–5); different PCR product sizes result from the use of different exon B return primers. In some experiments, the FN1ΔKKp and FN1ΔKB pre-mRNAs were spliced with slightly higher efficiency, as seen for FN1ΔKB in the F9 cell transfection studies (Fig. 1); the ΔKB deletion had a similar effect in FN5 (Fig. 4C, lane 2). IVS1 splicing was not substantially altered by the ΔKpS and ΔBS deletions in the context of FN3 (Fig. 4B, lanes 1–3) or the ΔKB deletion in the context of FN5 (Fig. 4C, lanes 1 and 3). We conclude that no single region of exon B is essential for IVS1 removal.

Analysis of the same splicing reactions for 7–8 joining revealed that exon B deletions did not alter the level of this spliced product (data not shown). When IVS2 removal was assessed, FN1ΔKKp and FN1ΔKB exhibited levels similar to the wild-type substrate (Fig. 4A, lanes 7–9). However, the ΔBS and ΔKpS deletions substantially reduced IVS2 removal in the context of FN1 (Fig. 4A, lanes 10 and 11) and FN3 (Fig. 4B, lanes 6 and 7), but not in the context of FN5 (Fig. 4C, lanes 5 and 6). The ΔBS deletion resulted in the formation of additional products corresponding to use of cryptic 5' splice sites. These results suggest that the deleted exon sequences are required for IVS2 splicing, specifically for accurate selection of the 5' splice site of FN1 and FN3, and use of the strong 5' splice site in FN5 did not require exon B sequences.

The mutated PREs in FN3mp had little effect on IVS1 removal (Fig. 4B, lane 4), but reduced correct B–8 joining (compare lanes 5 and 8), indicating involvement of both PREs in IVS2 removal. This suggests that the reduced level of B+ mRNA seen with FN3mp *in vivo* was the result of reduced IVS2 removal. A more quantitative determination of IVS2 splicing efficiency was achieved using the RNase protection assay (Fig. 3C). PCR products of incompletely spliced (IVS1–/IVS2+) and fully spliced (IVS1–/IVS2–) RNAs were quantified for FN3 and FN3mp. The ratio of incomplete to fully-spliced bands was 3:2 and 3:1 for FN3 and FN3mp respectively. This 50% decrease in fully-spliced FN3mp versus FN3 indicates that the PREs positively influence IVS2 splicing and play a role in exon B inclusion.

Spatial requirements for exon B sequences

The reduction of IVS2 splicing from the FN1ΔBS and FN3ΔBS pre-mRNAs was unexpected since PRE1 was present in these constructs. Inspection of the junction sequence resulting from the ΔBS deletion reveals that only 4 nt separate PRE1 and the 5' splice site, raising the possibility of a spatial dependence for PRE function. Polylinker sequences were inserted at the FN1ΔBS deletion junction to position PRE1 ~40 nt upstream of the 5' splice site, resembling the natural location of PRE2. Correct selection of the IVS2 5' splice site was partially restored by insertion of the spacer (Fig. 4A, compare lanes 11 and 12), although nearby cryptic sites were used as well. Thus, PRE1 does not appear to be as effective as PRE2 in selecting the proper 5' splice site or suppressing cryptic splice site use. In addition, the results suggest that PRE function is spatially constrained.

A heterologous ESE rescues 5' splice site selection and is position sensitive

A version of the cardiac troponin T (cTNT) exon 5 ESE containing the UP mutation (29) was inserted into exon B and splicing was performed *in vitro* (Fig. 5). This ESE is a purine-rich sequence tract (Pu_{24}) that stimulates use of the cTNT exon 5 3' splice site. Our manipulations positioned this ESE 23 nt downstream of the exon B 3' splice site (FN1cp) or 45 nt upstream of the exon B 5' splice site (FN1ΔBScp). The ESE at either position did not activate the exon B 3' splice site, as IVS1 removal was comparable for FN1cp, FN1ΔBScp and FN1 (Fig. 5, lanes 1 and 2 and Fig. 2B, lane 4). Instead, the ESE altered exon B 5' splice site use. For FN1cp, the ESE

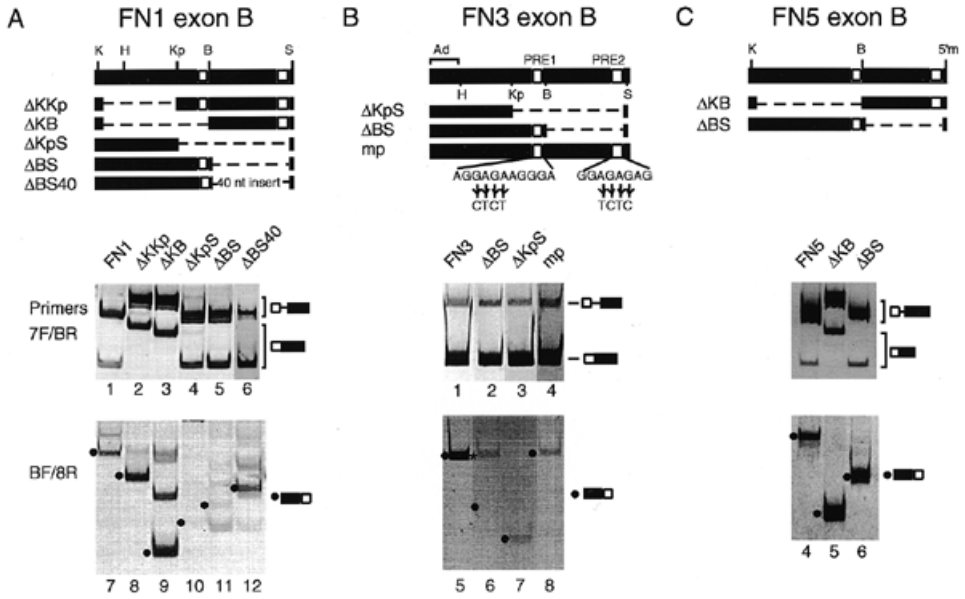

Figure 4. Exon B deletions interfere with proper IVS2 splicing. Regions deleted from exon B, dashed lines; PRE1 and PRE2, open squares in exon B. Pre-mRNA ΔBS40, 40 nt insertion at the ΔBS deletion site. Transversion mutations of four purine nucleotides in PRE1 and PRE2 are shown in (B). Products of *in vitro* splicing were detected by RT–PCR using indicated primers. IVS1 removal was assessed in reactions supplemented with 10 μg total SR proteins [(A), lanes 1–6; (B), lanes 1–4; (C), lanes 1–3]; for IVS2 removal, 5 μg total SR proteins were added [(A), lanes 7–12; (B), lanes 5–8; (C), lanes 4–6]. Bullets mark the expected position of correctly spliced B–8 products. (**A**) Splicing of FN1 and derivatives. Bands above the B–8 products in lanes 7–9 include a pseudo-exon in the middle of IVS2, a phenomenon observed at higher levels of SR proteins. (**B**) Splicing of pre-mRNA FN3 and derivatives. Asterisk (lane 6), band of unknown structure. (**C**) Splicing of FN5 and derivatives. This and subsequent figures are contrast-inverted images of ethidium bromide-stained gels.

stimulated use of exon B cryptic 5' splice sites (EC1, EC2 and EC3; Fig. 5, lane 3) which were identified by restriction site analysis and sequencing. Cryptic site EC2 corresponds to the site activated in F9 cells by the PRE mutations. The ESE in FN1ΔBScp activated the authentic exon B 5' splice site and a cryptic site in the intron (IC; Fig. 5, lane 4). These results indicate that the cTNT ESE activity was altered by the exon B context indicating that position and context are factors in ESE activity.

Accurate 5' splice site selection requires exon B sequences in a heterologous context

The above results suggest that PRE sequences in exon B facilitate use of the correct 5' splice site while disfavoring cryptic sites. Previous work has identified IVS2 sequences that are important for exon B inclusion (5,7). To test whether IVS2 sequences also contribute to exon B 5' splice site selection, exon B was inserted within the intron of adenovirus-derived construct PiP3 (28), along with a limited amount of flanking intron sequences (160 nt of IVS1 and 85 nt of IVS2) to generate AdFN. When AdFN was incubated in HeLa nuclear extract alone, joining of the flanking exons was observed with no exon B inclusion (Fig. 6, lanes 1, 6 and 11). Upon addition of SR proteins, splicing of both introns and three exon B+ product were detected (lanes 2, 7 and 12).

Deletion of exon B sequences did not alter IVS1 removal as compared with AdFN (Fig. 6, lanes 7–10). In addition, the ΔKpB deletion had no effect on splicing of IVS2 (compare lanes 12 and 13). However, the ΔKpS and ΔBS deletions reduced correct removal of IVS2 (lanes 14 and 15, also see lane 5). Restriction analyses and sequencing revealed that IVS2 of pre-mRNA AdFNΔBS was processed using three 5' splice sites: the authentic 5' splice site as well as cryptic sites EC1 and EC2. Pre-mRNA AdFNΔKpS gave rise to products that used either the authentic site or EC1. Thus, exon B deletions have the same deleterious effect on IVS2 splicing in this heterologous context as in the native context of pre-mRNA FN1 both *in vitro* and *in vivo*. Because of the limited amount of IVS1 and IVS2 sequences present in these constructs, it is likely that the exon sequences directly specify the correct exon B 5' splice site.

DISCUSSION

We have explored the mechanisms by which exon sequences and splice sites affect inclusion of alternative exon B *in vivo* and *in vitro*. We conclude that two purine-rich elements within exon B, PRE1 and PRE2, are required for proper 5' splice site selection, as revealed by reduced IVS2 removal and/or activation of cryptic 5' splice sites when these elements were deleted, mutated or repositioned. The requirement for these specific exon B sequences in proper 5' splice site selection was preserved in native and heterologous contexts *in vitro*. However, the PRE requirement was overridden by the insertion of a consensus 5' splice site, suggesting that the PRE dependence is linked to the suboptimal nature of the native 5' splice site. Thus, the balance between the exon sequences and the splice site may be important for the modulation of exon B splicing.

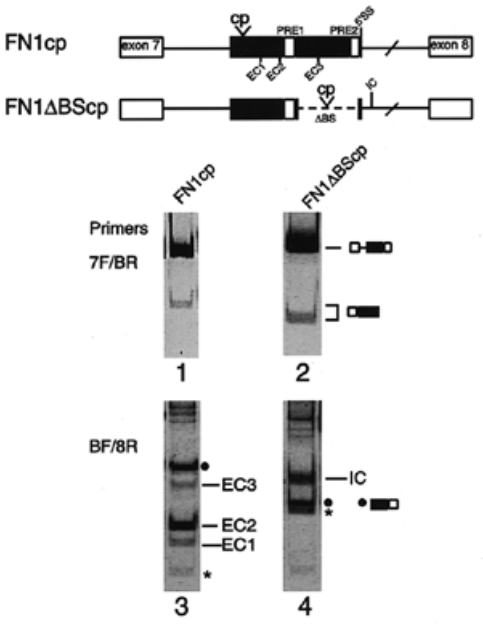

Figure 5. Heterologous ESE acts in a distance- and position-dependent manner. cp, cTNT ESE insertion sites. IVS1 (lanes 1 and 2) or IVS2 (lanes 3 and 4) removal was assessed by RT–PCR analysis of splicing reactions using indicated primers. Products generated from use of the correct exon B 5' splice site are noted by bullets. Asterisk, use of a cryptic 5' splice site internal to the consensus PRE.

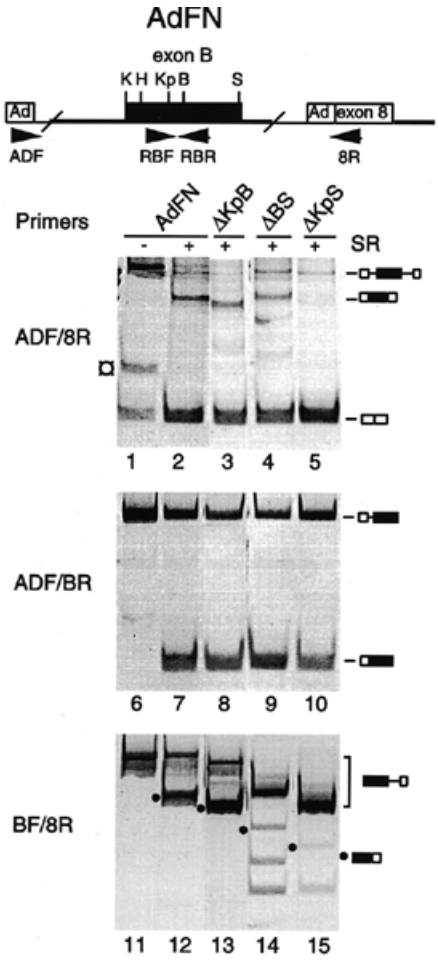

Figure 6. Exon B sequences influence 5' splice site selection in a heterologous context. AdFN and derivatives were spliced in HeLa nuclear extract with no SR protein (–) or 5 μg SR protein (+). RT–PCR detection of products was with indicated primer pairs. Bracketed circle, product of unknown structure. Bullets mark products spliced at the proper 5' splice site. Upper bands in lanes 6–15 are unspliced products. Additional bands in lanes 14 and 15 represent use of cryptic 5' splice sites.

The requirement for SR proteins exhibited by all of the FN sequences tested was surprising. The adenovirus-derived sequences of AdFN were active in nuclear extract alone (Fig. 6), as are other regions of the FN pre-mRNA (data not shown). Thus, it appears that SR protein dependence is a property specific to exon B and its flanking exons, although the mechanism of activation is not apparent. It is possible that the relative ratio of the SR proteins in the nuclear extract is not the same as in the purified preparations, which might affect splicing. Alternatively, the high levels of SR proteins might be needed to titrate out inhibitory factors present in the extract.

Mutation of individual PREs had little effect on splice site selection (data not shown), suggesting that the two elements might be redundant or cooperative. However, functional redundancy did not explain the lack of selector activity of the various ΔBS plasmids; either the upstream PRE1 was unable to substitute functionally for PRE2, or it was in an unfavorable position, since only 4 nt separated the last purine from the site of cleavage. Correct 5' splice site usage was restored by insertion of a spacer, favoring the latter explanation. Therefore, PRE1 can partially substitute for PRE2, although the use of cryptic splice sites suggests that PRE2 is stronger, and that PRE activity is position dependent. Another study also suggests that PRE2 is able to function alone, perhaps at a reduced efficiency (6). It remains possible that the ΔBS mutation moves an inhibitory sequence close to the 5' splice site, and the ΔBS40 insertion moves this putative inhibitor farther away. Such an inhibitor would need to act in the ΔKpS version of exon B as well and thus would lie over 30 nt upstream of the 5' splice site. We favor the interpretation that PRE activity is affected by both sequence and position with respect to the 5' splice site.

Coordinated recognition of both ends of the exon as predicted by the exon definition model (40) predicts that improvement of a single splice site can increase the splicing of both introns that flank the exon. Experimental evidence supports this prediction (reviewed in 24). In transfection experiments, exon B appeared to conform to an exon-based mode of recognition, as improvement of either splice site resulted in a high level of inclusion *in vivo*. Detailed investigation using our *in vitro* splicing assay revealed that activation of exon B inclusion resulting from an improved 3' splice site region was due to increased splicing of IVS1, not IVS2; similarly, an improved 5' splice site mainly increased splicing of IVS2, with less effect on IVS1. We postulate that each splice site substitution acts by increasing splicing of the intron that includes the altered site, decreasing use of the competing exon-skipping pathway. Thus, both weak exon B splice sites restrict exon inclusion, and may be recognized independently by the splicing apparatus.

Analysis of deletion mutants indicated that exon B sequences did not reveal enhancer activity with respect to IVS1. This is in contrast to the situation for β-tropomyosin exon 6, in which exon sequences affect usage of both flanking splice sites, apparently by facilitating a bridging interaction (41). However, our results with the ΔKKp and ΔKB mutations suggest a repressor activity may lie in the 5' portion of exon B. Similar findings have been reported (3,6). The critical sequences that influence use of the 3' splice site have not been identified and our results do not exclude repositioning a positive element. A similarly positioned splicing suppressor has been identified in FN alternative exon A, which relies on secondary structure for activity (42). Sequences within the 5' portion of exon B also are predicted to assume a higher order structure (not shown), although the relevance to possible splicing suppressor activity is unknown.

The potential complexity of splice site activation by purine-rich sequences is well illustrated by a sequence element that lies between two alternative 5' splice sites within an internal exon of the caldesmon gene. This element is required for selection of the upstream 5' splice site (18), but appears to have no effect on the downstream site. However, substitution of the native caldesmon PRE with the cTNT exon 5 ESE results in preferential selection of the downstream 5' splice site (43). Therefore, for both caldesmon and fibronectin pre-mRNAs, cTNT ESE activity is strongly influenced by the local sequence context. In addition, our results revealed an additional unexpected activity of the exon B PREs: the suppression of nearby cryptic 5' splice sites.

The principle determinant of 5' splice site selection is complementarity to U1 snRNA. On this basis, the exon B 5' splice site should be preferred to any of the cryptic sites, as it is a better match to the consensus. However, evidence also implicates SR proteins in selection of 5' splice sites, especially alternative sites (38,44–46). We have used UV cross-linking to establish that SRp40 binds to PRE1 and SRp20 binds to PRE2 (see Supplementary Material); others have also reported the former interaction (6). The relevance of these interactions to 5' splice site selection remains to be established.

SUPPLEMENTARY MATERIAL

See Supplementary Material available in NAR Online.

ACKNOWLEDGEMENTS

We dedicate this manuscript to the memory of Vickie D. Bennett. We are grateful to M. Aros for excellent technical assistance and to R. Fishel for helpful discussions and critical reading of the manuscript. This work was supported by a grant from the National Institute of General Medical Sciences (R01-GM47453) to P.A.N.

REFERENCES

1. Hynes,R.O. (1990) *Fibronectins.* Springer-Verlag, New York.
2. ffrench-Constant,C. (1995) *Exp. Cell Res.*, **221**, 261–271.
3. Huh,G.S. and Hynes,R.O. (1993) *Mol. Cell. Biol.*, **13**, 5301–5314.
4. Norton,P.A. and Hynes,R.O. (1990) *Nucleic Acids Res.*, **18**, 4089–4097.
5. Huh,G.S. and Hynes,R.O. (1994) *Genes Dev.*, **8**, 1561–1574.
6. Du,K., Peng,Y., Greenbaum,L.E., Haber,B.A. and Taub,R. (1997) *Mol. Cell. Biol.*, **17**, 4096–4104.
7. Lim,L.P. and Sharp,P.A. (1998) *Mol. Cell. Biol.*, **18**, 3900–3906.
8. Moore,M.J., Query,C.C. and Sharp,P.A. (1993) In Gesteland,R. and Atkins,J. (eds), *The RNA World*. Cold Spring Harbor Laboratory Press, Cold Spring Harbor, NY, pp. 303–358.
9. Sharp,P.A. (1994) *Cell*, **77**, 805–815.
10. Madhani,H.D. and Guthrie,C. (1994) *Genes Dev.*, **8**, 1071–1086.
11. Steitz,J.A. (1992) *Science*, **257**, 888–889.
12. Mardon,H.J., Sebastio,G. and Baralle,F.E. (1987) *Nucleic Acids Res.*, **15**, 7725–7733.
13. Ryan,K.J. and Cooper,T.A. (1996) *Mol. Cell. Biol.*, **16**, 4014–4023.
14. Watakabe,A., Tanaka,K. and Shimura,Y. (1993) *Genes Dev.*, **7**, 407–418.
15. Wang,J. and Manley,J.L. (1995) *RNA*, **1**, 335–346.
16. Tian,M. and Maniatis,T. (1994) *Genes Dev.*, **8**, 1703–1712.
17. Sun,Q., Mayeda,A., Hampson,R.K., Krainer,A.R. and Rottman,F.M. (1993) *Genes Dev.*, **7**, 2598–2608.
18. Humphrey,M.B., Bryan,J., Cooper,T.A. and Berget,S.M. (1995) *Mol. Cell. Biol.*, **15**, 3979–3988.
19. Caputi,M., Casari,G., Guenzi,S., Tagliabue,R., Sidoli,A., Melo,C.A. and Baralle,F.E. (1994) *Nucleic Acids Res.*, **22**, 1018–1022.
20. Amendt,B.A., Si,Z.H. and Stoltzfus,C.M. (1995) *Mol. Cell. Biol.*, **15**, 4606–4615.
21. Del Gatto,F. and Breathnach,R. (1995) *Mol. Cell. Biol.*, **15**, 4825–4834.
22. Valcárcel,J. and Green,M.R. (1996) *Trends Biochem. Sci.*, **21**, 296–301.
23. Chabot,B. (1996) *Trends Genet.*, **12**, 472–478.
24. Berget,S.M. (1995) *J. Biol. Chem.*, **270**, 2411–2414.
25. Hoffman,B.E. and Grabowski,P.J. (1992) *Genes Dev.*, **6**, 2554–2568.
26. Wu,J.Y. and Maniatis,T. (1993) *Cell*, **75**, 1061–1070.
27. Talerico,M. and Berget,S.M. (1990) *Mol. Cell. Biol.*, **10**, 6299–6305.
28. Garcia-Blanco,M.A., Jamison,S.F. and Sharp,P.A. (1989) *Genes Dev.*, **3**, 1874–1886.
29. Ramchatesingh,J., Zahler,A.M., Neugebauer,K.M., Roth,M.B. and Cooper,T.A. (1995) *Mol. Cell. Biol.*, **15**, 4898–4907.
30. Chomczynski,P. and Sacchi,N. (1987) *Anal. Biochem.*, **162**, 156–159.
31. Dignam,J.D., Lebovitz,R.M. and Roeder,R.G. (1983) *Nucleic Acids Res.*, **11**, 1475–1489.
32. Zahler,A.M., Lane,W.S., Stolk,J.A. and Roth,M.B. (1992) *Genes Dev.*, **6**, 837–847.
33. Kuo,B.A., Gonzalez,I.L., Gillespie,D.A. and Sylvester,J.E. (1996) *Nucleic Acids Res.*, **24**, 4817–4824.
34. Strickland,S., Smith,K.K. and Marroti,K.R. (1980) *Cell*, **21**, 347–355.
35. Wang,Y.-C., Selvakumar,M. and Helfman,D.M. (1997) In Krainer,A.R. (ed.), *Eukaryotic mRNA Processing.* IRL Press, Oxford, pp. 242–279.
36. Norton,P.A. (1994) *Nucleic Acids Res.*, **22**, 3854–3860.
37. Barone,M.V., Henchcliffe,C., Baralle,F.E. and Paolella,G. (1989) *EMBO J.*, **8**, 1079–1085.
38. Krainer,A.R., Conway,G.C. and Kozak,D. (1990) *Cell*, **62**, 35–42.
39. Ge,H. and Manley,J.L. (1990) *Cell*, **62**, 25–34.
40. Robberson,B.L., Cote,G.J. and Berget,S.M. (1990) *Mol. Cell. Biol.*, **10**, 84–94.
41. Selvakumar,M. and Helfman,D.M. (1999) *RNA*, **5**, 378–394.
42. Staffa,A., Acheson,N.H. and Cochrane,A. (1997) *J. Biol. Chem.*, **272**, 33394–33401.
43. Elrick,L.L., Humphrey,M.B., Cooper,T.A. and Berget,S.M. (1998) *Mol. Cell. Biol.*, **18**, 343–352.
44. Zahler,A.M. and Roth,M.B. (1995) *Proc. Natl Acad. Sci. USA*, **92**, 2642–2646.
45. Horowitz,D.S. and Krainer,A.R. (1994) *Trends Genet.*, **10**, 100–106.
46. Eperon,I.C. (1993) *EMBO J.*, **12**, 3607–3617.